Journal of Alloys and Compounds 667 (2016) 310–316

Contents lists available at ScienceDirect

Journal of Alloys and Compounds

journal homepage: http://www.elsevier.com/locate/jalcom

The intermediate phase and low wavenumber phonon modes in antiferroelectric $(Pb_{0.97}La_{0.02})(Zr_{0.60}Sn_{0.40-y}Ti_y)O_3$ ceramics discovered from temperature dependent Raman spectra

Xiaojuan Ding [a], Shuang Guo [a], Zhigao Hu [a, *], Xuefeng Chen [b], Genshui Wang [b], Xianlin Dong [a], Junhao Chu [a]

[a] Department of Electronic Engineering, East China Normal University, Shanghai 200241, China
[b] Key Laboratory of Inorganic Functional Materials and Devices, Shanghai Institute of Ceramics, Chinese Academy of Sciences, 1295 Dingxi Road, Shanghai 200050, China

ARTICLE INFO

Article history:
Received 1 October 2015
Received in revised form
13 January 2016
Accepted 24 January 2016
Available online 27 January 2016

Keywords:
Ferroelectrics
Phase transitions
Low wavenumber phonon modes
Intermediate phase

ABSTRACT

Optical phonons and phase transitions of $(Pb_{0.97}La_{0.02})(Zr_{0.60}Sn_{0.40-y}Ti_y)O_3$ (PLZST 97/2/60/40-100y/100y) ceramics with different compositions have been investigated by x-ray diffraction and temperature dependent Raman spectra. From the temperature dependence of low wavenumber phonon modes, two phase transitions (antiferroelectric orthorhombic to intermediate phase and intermediate phase to paraelectric cubic phase) were detected. The intermediate phase could be the coexistence one of antiferroelectric orthorhombic and ferroelectric rhombohedral phase. In addition, two modes (a soft mode and an anharmonic hopping central mode) were found in the high temperature paraelectric cubic phase. On cooling, the anharmonic hopping central mode splits into two modes in the terahertz range. Moreover, the antiferrodistortive mode appears in the antiferroelectric orthorhombic phase. Based on the analysis, the phase diagram of PLZST ceramics can be well improved.

1. Introduction

Lead zirconate titanate (PZT) system as a typical perovskite material has been widely used in sensors and actuators due to its high piezoelectric and coupling coefficients first measured by Berlincourt et al [1]. The phase diagram of PZT system determined by Jaffe et al. shows a rich phase distribution [2]. The titanate (Ti)-rich parts of the phase diagram are ferroelectric tetragonal (FE_T) phase with $P4mm$ symmetry. Additionally several more complex phase boundaries occur on the zirconate (Zr)-rich side. The ferroelectric rhombohedral (FE_R) structure at high temperature has space group with $R3m$ symmetry, which indicates that the average cation displacements are along the $[111]_p$ direction (where p = pseudocubic). A phase transition to $R3c$ occurs on cooling as a result of antiphase tilting of the oxygen octahedra about the $[111]_p$ axis [3]. Close to the $PbZrO_3$ end, a phase boundary between FE_R with $R3m$ symmetry and antiferroelectric orthorhombic (AFE_O) with $Pbam$ symmetry is encountered.

Nowadays the phase transitions between AFE_O and FE_R phases of the pure and Zr-rich compositionally modified $PbZrO_3$ have been intensively studied by many workers by means of structural, dielectric, pyroelectric, piezoelectric, and optical investigations [4–9]. Several new phases located close to the AFE_O and FE_R phase boundaries have been identified in the PZT phase diagram [10–12]. As we know, the stability of the AFE_O and FE_R phases can be altered through the chemical substitutions of La^{3+} at the Pb site and Ti^{4+} or Sn^{4+} at the Zr site. Thus, it could easily produce several new phases and generate a rich phase picture by modification. Additionally, it was reported that some new phases could be induced by the substitution of Sn^{4+} for Zr^{4+} when the composition of Sn exceeds 30%. These new phases were considered to be ferroelectric and antiferroelectric phases or the coexistence of both phases [11]. Nowadays we discovered a transient phase in $(Pb_{0.97}La_{0.02})(Zr_{0.60}Sn_{0.40-y}Ti_y)O_3$ (PLZST, $2.0\% \le y \le 6.0\%$) ceramics, where the low wavenumber phonon modes present an abrupt variation with the temperature. Note that the new phase may be the intermediate phase. As we know, the phase transformations are associated with lattice variations, consequently resulting in the changes of phonon modes. Fortunately, Raman scattering as a nondestructive and

* Corresponding author.
E-mail address: zghu@ee.ecnu.edu.cn (Z. Hu).

http://dx.doi.org/10.1016/j.jallcom.2016.01.188
0925-8388/

readily available characterization technique has been widely used to study structural phase transitions in ferroelectric system.

In this article, the phase transitions and low wavenumber phonon modes of $(Pb_{0.97}La_{0.02})$ $(Zr_{0.60}Sn_{0.40-y}Ti_y)O_3$ ceramics have been investigated through x-ray diffraction (XRD) and temperature dependent Raman scattering. Based on the variations of low wavenumber phonon modes, the new phase which we call the intermediate phase was also observed. We review the evidence for the intermediate phase and present an overview of the structural variations which occur near the boundary between the AFE_O and FE_R phase.

2. Experimental details

The $(Pb_{0.97}La_{0.02})$ $(Zr_{0.60}Sn_{0.40-y}Ti_y)O_3$ (PLZST, $2.0\% \leq y \leq 6.0\%$) ceramics were fabricated by a conventional solid–state reaction sintering, using the appropriate amount of reagent grade raw materials of lead tetraoxide (Pb_3O_4), zirconium dioxide (ZrO_2), titanium dioxide (TiO_2), tin oxide (SnO_2), and lanthanum oxide (La_2O_3). The sintering process was carried out in a lead rich environment in order to minimize lead volatilization. The samples were sintered at 1300 °C for 1 h in air atmosphere. The details of fabricating process can be found in Ref. [4]. Before spectral measurements, the ceramics with the diameter of 15 mm and the thickness of 1 mm were rigorously single-side polished and cleaned in pure ethanol with an ultrasonic bath and rinsed several times by deionized water. The crystalline structures of the PLZST ceramics were investigated by XRD at room temperature using a Ni filtered Cu-Kα radiation operated at 40 kV and 200 mA (D/MAX-2550V, Rigaku Co.). In the XRD experiments, a vertical goniometer (model RINT2000) was used, and continuous scanning mode ($2\theta/\theta$) was selected with an interval of 0.02°. The 2θ range was 20–80° and the scanning rate was 10° min^{-1}. On the other hand, temperature dependent Raman scattering measurements were carried out by a Jobin-Yvon LabRAM HR 800 UV micro-Raman spectrometer and a THMSE 600 heating/cooling stage (Linkam Scientific Instruments) in the temperature range from 100 to 650 K with a resolution of 0.1 K. The He–Ne laser with the wavelength of 632.8 nm is taken as the exciting source, which is believable for recording low wavenumber Raman phonon modes and the signal is very good. The laser beam was focused

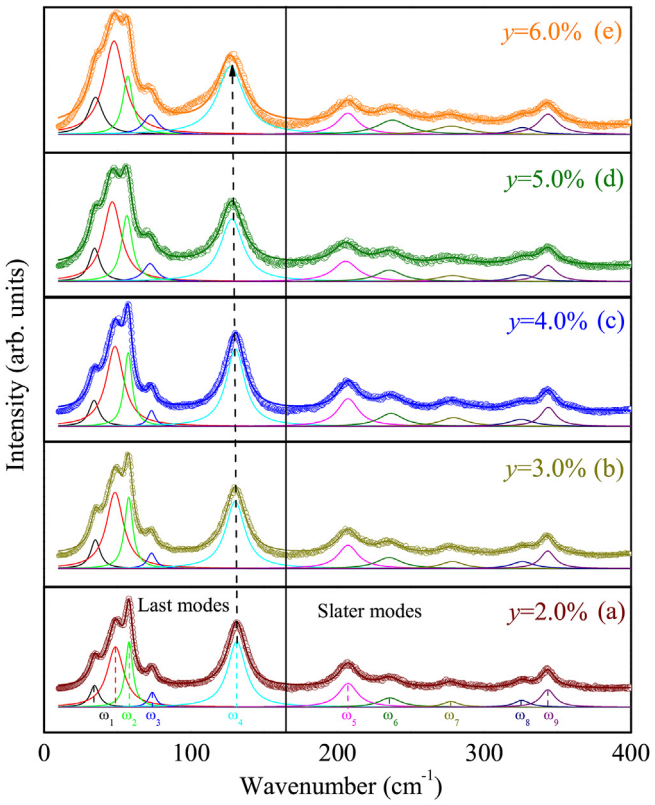

Fig. 2. Raman spectra of PLZST ceramics with different Ti composition at 100 K and the corresponding harmonic oscillator fitting results. Note that the dashed lines are applied to guide the eyes.

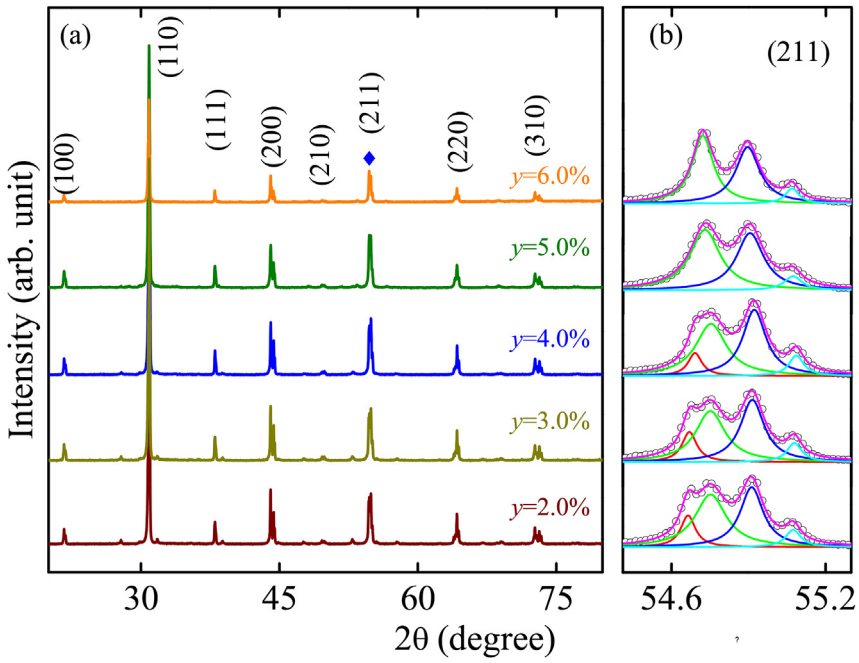

Fig. 1. (a) X-ray diffraction patterns of $(Pb_{0.97}\ La_{0.02})$ $(Zr_{0.60}\ Sn_{0.40-y}\ Ti_y)O_3$ ceramics with different Ti composition recorded at room temperature. (b) The enlarged regions for the diffraction peaks (211) at $2\theta \approx 55^{\circ}$.

through a 50× microscope with a working distance of 18 mm. An aircooled charge coupled device (CCD) (−70 °C) with a 1024 × 256 pixels front illuminated chip was used to collect the scattered signal dispersed on 1800 grooves/mm grating. To get rid of the trivial temperature dependence, all Raman spectra have been divided by the Bose-Einstein occupation number $n(\omega) + 1 = 1/[1 - \exp(-\hbar\omega/k_BT)$ ($\hbar$ and k_B are Planck constant and Boltzmann constant, respectively) [15]. Note that the derived Raman spectra can be fitted with independent Lorentzian damped harmonic oscillators to uniquely obtain the phonon wavenumber [17–19].

3. Results and discussion

3.1. Structural analysis

Fig. 1(a) shows the XRD patterns of the PLZST ceramics at room temperature. The strongest (110) diffraction peak is located at about 31° and other weaker peaks (100), (111), (200), (210), (211), (220), and (310) also appear. It indicates that the ceramics are of pure perovskite structure and there is no secondary pyrochlore structure. The patterns show high similarity to those of single crystal powder [14], which suggests good quality of PLZST ceramics. The enlarged regions for the diffraction peak (211) at $2\theta \approx 55°$ are presented in Fig. 1(b). For PLZST ceramics with $y = 2\%$, the (211) peak was fitted with four Lorentzians. While for PLZST with $y = 4\%$, the left-most peak merges into the nearest one and becomes the shoulder structure. Further increasing the composition of Ti to 5%, the left-most peak disappears, which indicates that there is a phase transition although the variation is small.

3.2. Raman spectroscopic analysis as a function of temperature

Raman scattering results and well-fitted deconvolution peaks at 100 K for $(Pb_{0.97}La_{0.02})(Zr_{0.60}Sn_{0.40-y}Ti_y)O_3$ ceramics are depicted in Fig. 2. All of the spectra can be divided into two main bands of cubic ABO_3 perovskite materials, with the wavenumber range from 10 to 160 cm^{-1} labeled as Last modes and from 160 to 400 cm^{-1} labeled as Slater modes, respectively. The eigenvectors of these modes are mainly related to the A-, and B-cation displacements, respectively [16]. The Last modes are fitted with five independent harmonic oscillators, with the anharmonic hopping central mode (ω_1) located at about 34 cm^{-1} and 49 cm^{-1}, ω_2 mode at 59 cm^{-1}, the antiferrodistortive mode (ω_3) at 73 cm^{-1}, and ω_4 mode at 130 cm^{-1}, respectively. It is seen that the left ω_1 mode (34 cm^{-1}) becomes a shoulder structure with increasing the composition of Ti. Additionally, the ω_4 mode was observed to shift to lower wavenumber from Fig. 2, which can be attributed to the decrease of electronegativity by the substitution of Ti^{4+} for Sn^{4+}. For the Slater modes, five independent harmonic oscillators can also be used to fit, with ω_5 mode at 207 cm^{-1}, ω_6 mode at 236 cm^{-1}, ω_7 mode at 277 cm^{-1}, ω_8 mode at 325 cm^{-1}, and ω_9 mode at 343 cm^{-1}, respectively. Note that the assignments of phonon modes are labeled at the bottom of PLZST with $y = 2\%$ in Fig. 2 and also comprehensively listed in Table 1. One can see that Raman spectra for PLZST ceramics are similar to these for $PbZrO_3$, which indicates that our samples are really located at the boundary between AFE_O and FE_R [20]. Additionally, compared to Raman spectra of $Pb(Zr_{0.65}Sn_{0.35})O_3$ at room temperature presented by Jankowska-Sumara [11], extral phonon modes are present in our spectra, such as the low wavenumber Last phonon modes. These extral phonon modes could be due to the doping of La and Ti, which reduces the lattice structure symmetry.

To elucidate the thermal evolution of $(Pb_{0.97}La_{0.02})(Zr_{0.60}Sn_{0.40-y}Ti_y)O_3$ ceramics, temperature dependence of Raman spectra from 100 to 650 K are shown in Fig. 3. For better to present the figure, PLZST ceramics with $y = 3\%$ has not been shown. On heating, all modes from four samples become more flat and some of them disappear above 400 K, which shows the presence of "true" cubic system. It indicates that there is a phase transformation to PE_C at the temperature of about 400 K, which agrees well with the decrease of Raman intensity while increasing temperature in Fig. 4. As we know, the fact that the significant intensity decreases with increasing temperature indicates that the symmetry evolves continuously towards the high one (the paraelectric cubic phase) [21,22]. Here we must point out that some Raman modes are still present in the cubic phase, despite the forbidden selection rules, as it is well known for many Pb-based relaxor ferroelectric materials. The presence of Raman-active modes could be ascribed to local unit cell doubling and symmetry breakdown due to the off-site cations [13,20]. Additionally, all modes present a shift towards lower wavenumbers compared to those at 100 K, which can be due to thermal expansion of lattice [23]. In detail, the ω_1 mode at about 34 cm^{-1}, having its origin in anharmonic Pb atom vibrations (hopping among the available off center sites) becomes a shoulder structure and eventually merges into the mode at 49 cm^{-1}. One of the contributions is the reduce of structural symmetry. For the mode in the range of 52–58 cm^{-1}, it is assigned to the ω_2 mode, deriving from the F_{1u} mode in the PE_C phase. It was reported that vibrations of the Pb atom against the octahedra network in the direction perpendicular to the spontaneous polarization, which is expected to the main component of the soft mode of the ferroelectric transitions [4,24]. In addition, we can see that the ω_3 mode related to the antiferrodistortive R_{25} mode (tilt of the oxygen octahedra about the polarization axis) disappears on heating. The existence of this mode has been verified by a small dielectric peak in the permittivity from PZT with high Zr content [25]. It was reported that this mode stems from the Brillouin zone corner where

Table 1
The assignments of symmetries from the fitting deconvolution peaks in Raman scattering of PLZST ceramics with y = 2% recorded at 100 K, T^*, and T_C. Note that the unit of the phonon wavenumber is cm^{-1} and the error bars are presented in parentheses.

Symmetry (100 K)	AFE_O					Pbam			
Phonon modes	ω_1	ω_2	ω_3	ω_4	ω_5	ω_6	ω_7	ω_8	ω_9
	34.4/48.6 (0.1/0.1)	57.9 (0.1)	73.8 (0.1)	131.3 (0.1)	207.2 (0.1)	235.6 (0.3)	277.3 (0.5)	325.6 (0.4)	343.3 (0.2)
Symmetry (T^*)			Intermediate phase			Pbam and R3m			
	36.7 (0.2)	52.6 (0.6)	– (–)	101.1 (0.2)	211.2 (1.4)	236.7 (1.5)	267.3 (1.2)	325.6 (1.2)	335.8 (0.8)
Symmetry (T_C)			PE_C			Pm3m			
	36.5 (0.4)	58.7 (0.4)	– (–)	83.4 (0.8)	216.0 (1.8)	240.4 (1.5)	271.4 (1.9)	326.1 (2.9)	336.1 (3.0)

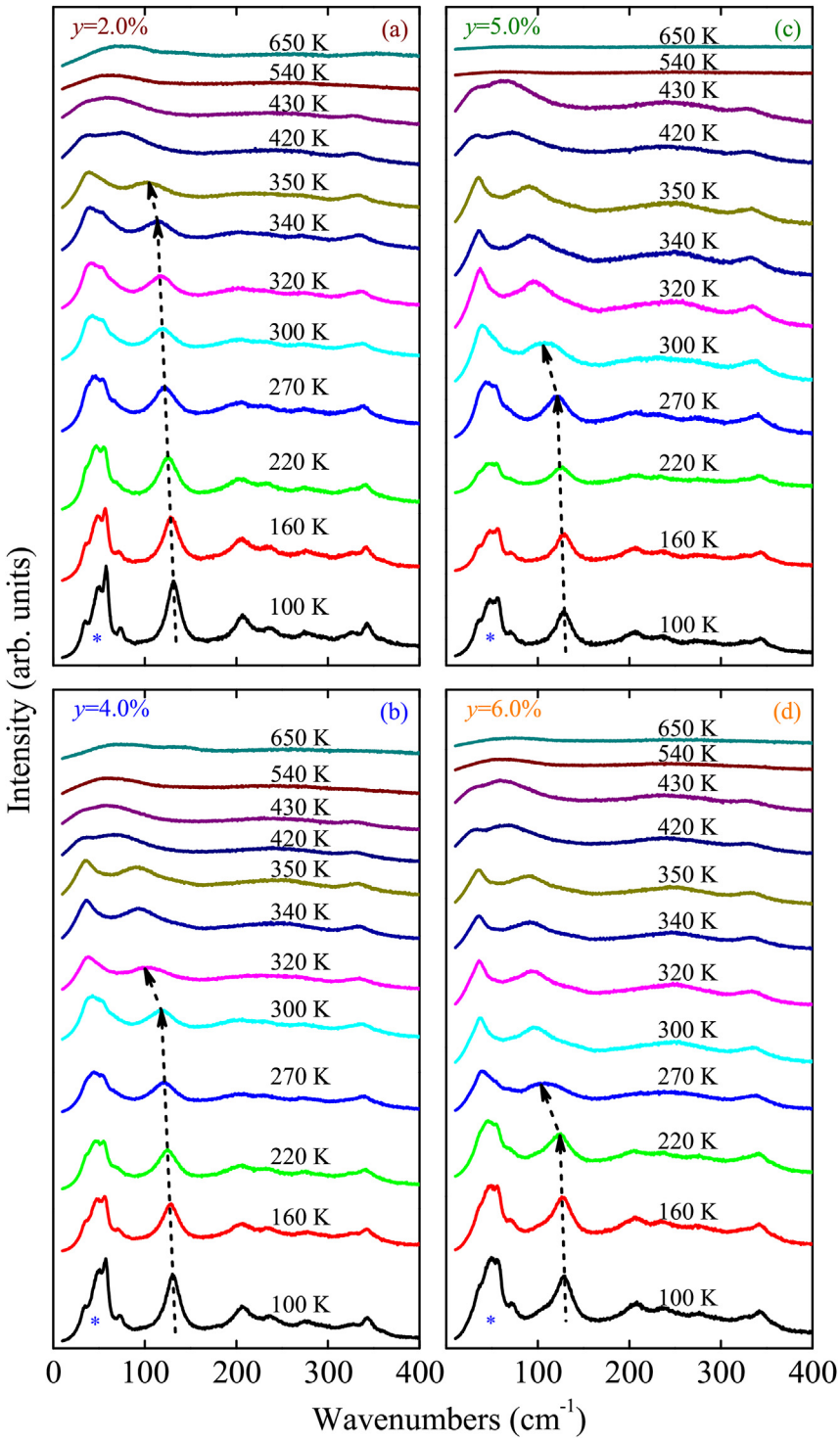

Fig. 3. Temperature dependent Raman spectra for PLZST ceramics from 100 to 650 K. The symbol (*) represents the low wavenumber phonon modes. Note that the dashed lines are applied to guide the eyes.

it is nonpolar. However, in the doubled unit cell, it can be activated by the Pb—O interaction, as shown by the dynamical simulations [26]. The ω_4 mode stemming from splitting of T_{1u} in PE_C phase is considered to consist of displacements of the B-cation and oxygen ions relative to Pb^{2+} ions in PZT [27]. It softens more than other modes on heating, which indicates that the ω_4 mode is more susceptible to the temperature and there is a phase transformation during the heating process. As we know, the anomalous behavior of the peak position is directly related to the phase transition mechanism [28]. Thus, the abrupt variations of low wavenumber phonon modes demonstrate a phase transition on the heating process.

To further investigate the phase transition mechanism, we plot temperature dependence of the wavenumber from ω_4, ω_3, ω_2, and ω_1 modes in Fig. 5. Two phase transition regions can be easily recognized based on the abrupt variations of low wavenumber phonon modes. On heating to the temperature of about 300 K, a

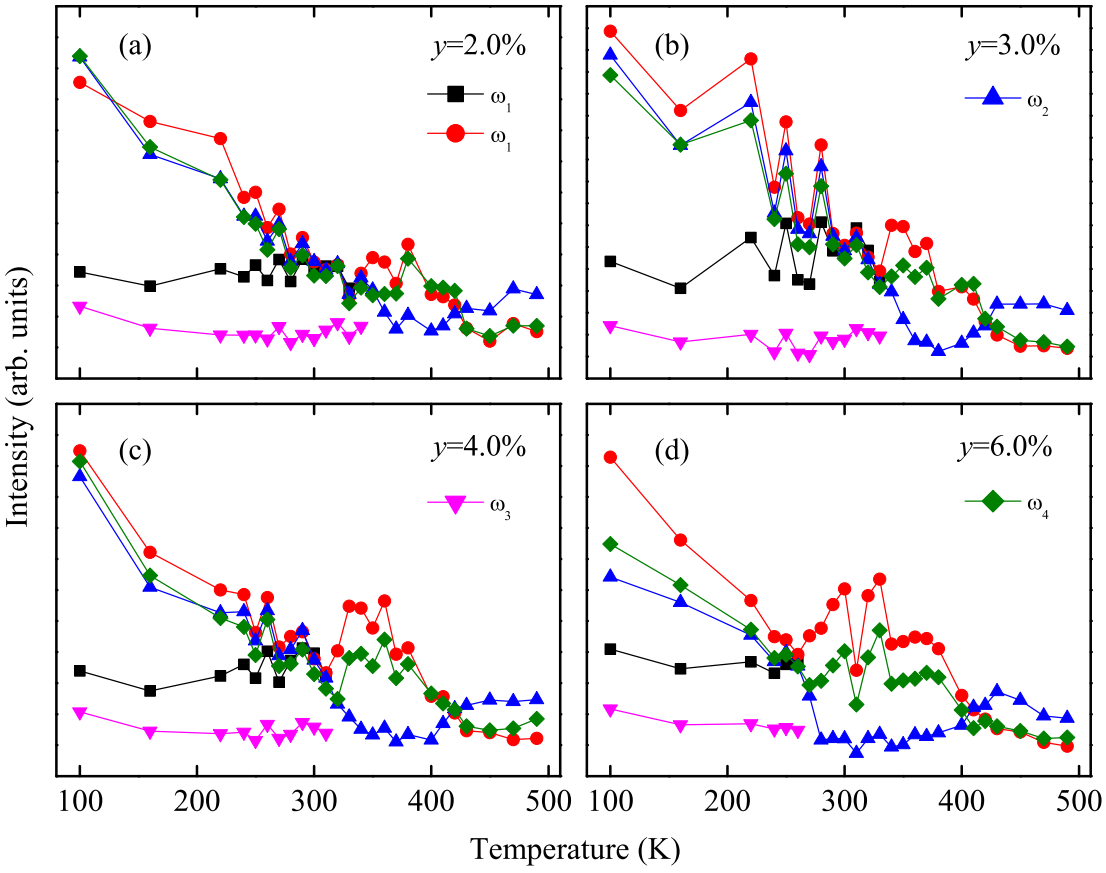

Fig. 4. Temperature dependence of Raman intensity of PLZST ceramics.

new transient phase which we call the intermediate phase was observed. For pure PZT ceramics, the intermediate phase has been confirmed by superlattice reflections and transmission electron microscopy [10]. It has a new lower symmetry cell unit with space group *Pm* compared to *Pbam*. This space group does not allow tilting to occur but does allow the Pb^{2+} ions to displace with the same vectors as in the *Pc* model. For the appearance of the intermediate phase, there are two reasons. Firstly, since our samples are located near the boundary between AFE_O and FE_R phase and both of these phases have very close free energy, it is possible for the intermediate phase to be induced by increasing temperature and doping of foreign ions. In addition, it is known that increasing temperature and doping can introduce defects. So the intermediate phase does not appear spontaneously but is induced by defects. Secondly, phase transformations of Zr-rich regions are frustrated by the surrounding matrix and consequently adopt a structure that is intermediate between AFE_O and FE_R phase. The volume fraction of the intermediate phase logically increases as the Ti concentration decreases until they are of sufficient size and number to stabilize the AFE_O *Pbam*. For the phase composition of the intermediate phase, it is not the pure AFE_O or FE_R phase but the coexistence of both phases due to the competition between AFE_O and FE_R phases.

3.3. Phase diagram of PLZST ceramics

Based on the temperature dependence of low wavenumber phonon modes, the phase diagram of PLZST ceramics can be presented in Fig. 6. It can be divided into three parts, with the intermediate phase observed a narrow temperature range between AFE_O and PE_C phase. At room temperature, we can see that the PLZST ceramics go through a transformation from AFE_O to the intermediate phase when the composition of Ti exceeds 5.0%, which is consistent with the results from XRD. Furthermore, it is worth noticing that the samples undergo successive phase transitions as increasing temperature. In detail, for PLZST with $y = 2.0\%$, there is a phase transition from the AFE_O to the intermediate phase at T^* of about 350 K. On further heating, the intermediate phase becomes instable and transfers to PE_C phase at T_C of about 420 K. While compared to pure PZT materials, T_C for our samples is lower, which can be ascribed to the doping of La and Sn [13,29]. Note that the boundaries in the phase diagram should not be taken rigorously. It is because the phase coexistence may occur over a relatively wide temperature region.

4. Conclusion

To summarize, the phase transitions and thermal evolutions of PLZST ceramics have been investigated by XRD and temperature dependent Raman spectra. It was found that two modes (a soft mode and an anharmonic hopping central mode) appear in high temperature PE_C phase. On cooling, the AHC mode splits into two modes in the terahertz range. Moreover, the antiferrodistortive mode occurs in the AFE_O phase. Based on the low wavenumber phonon modes variations, the phase diagram can be well improved. In addition, a new transient phase called the intermediate phase was found to exist between AFE_O and PE_C phase, which could be induced by defects through increasing temperature and doping of foreign ions.

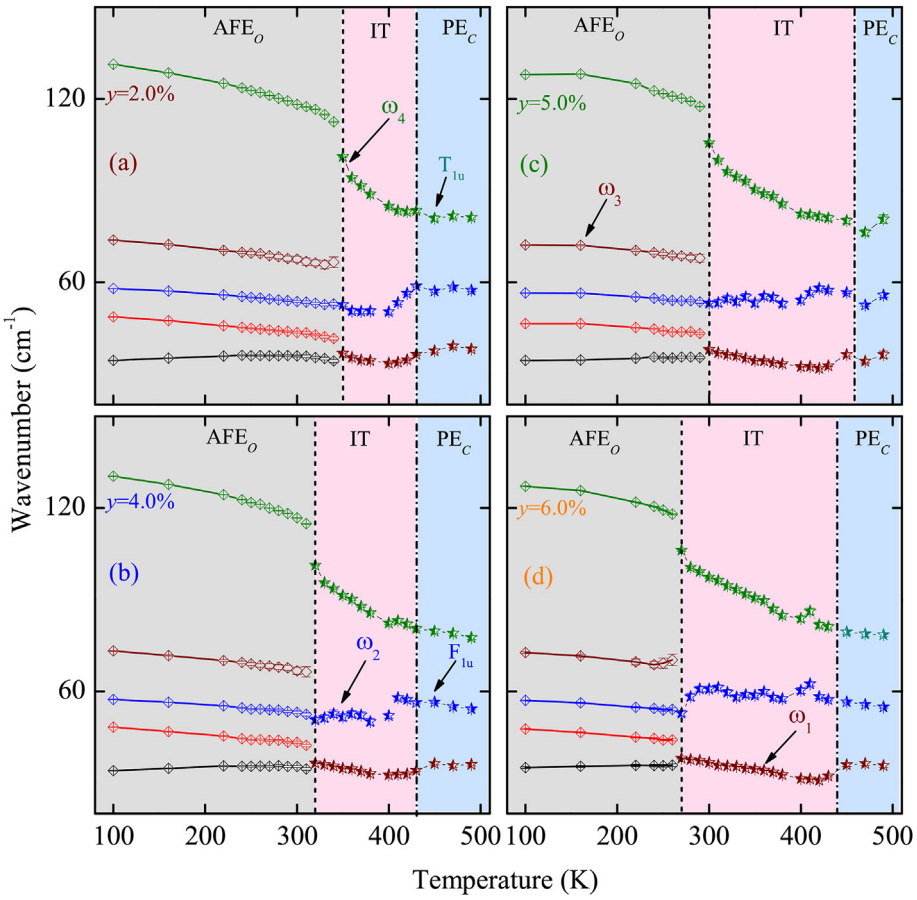

Fig. 5. The variations of $A_1(TO_1)$, AFD, $E(TO_1)$, and AHC modes as a function of temperature for PLZST ceramics with different Ti composition. Note that the dashed lines show the boundaries of two adjacent phase structures.

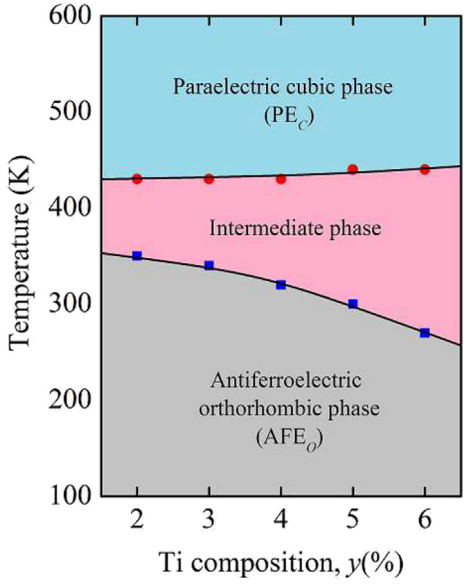

Fig. 6. The phase diagram of PLZST ceramics based on the low wavenumber phonon mode variations with the temperature and Ti composition. The phase transformation regions of AFE_O, intermediate phase and PE_C characteristics can be clearly distinguished by the solid dots.

Acknowledgments

One of the authors (X. J. Ding) would like to thank Drs. Zhihua Duan, Xiao Chen and Pengpeng Jiang for constructive discussions. This work was financially supported by Major State Basic Research Development Program of China (Grant Nos. 2011CB922200 and 2013CB922300), Natural Science Foundation of China (Grant Nos. 11374097 and 61376129), Projects of Science and Technology Commission of Shanghai Municipality (Grant Nos. 15JC1401600, 14XD1401500, 13JC1402100, and 13JC1404200), and the Program for Professor of Special Appointment (Eastern Scholar) at Shanghai Institutions of Higher Learning.

References

[1] D. Berlincourt, Transducers using forced transitions between ferroelectric and antiferroelectric states, IEEE Trans. Sonics Ultrason. 13 (1966) 116.
[2] B. Jaffe, W.R. Cook, H. Jaffe, Piezoelectric Ceramics, Academic Press, London, 1971.
[3] A.M. Glazer, Simple ways of determining perovskite structures, Acta Crystallogr. Sect. A Cryst. Phys. Diffr. Theor. Gen. Crystallogr. 31 (1975) 756.
[4] E. Buixaderas, I. Gregora, M. Savinov, J. Hlinka, L. Jin, D. Damjanovic, B. Malic, Compositional behavior of Raman-active phonons in $Pb(Zr_{1-x}Ti_x)O_3$ ceramics, Phys. Rev. B 91 (2015) 014104.
[5] J. Hlinka, T. Ostapchuk, E. Buixaderas, C. Kadlec, P. Kuzel, I. Gregora, J. Kroupa, M. Savinov, A. Klic, J. Drahokoupil, Multiple soft-mode vibrations of lead zirconate, Phys. Rev. Lett. 112 (2014) 197601.
[6] E. Buixaderas, T. Ostapchuk, J. Kroupa, M. Savinov, I. Gregora, J. Hlinka, Catching the intermediate phase in PZT 99/1 single crystals, Phase Trans. 87 (2014) 1105–1113.
[7] F. Cordero, F. Trequattrini, F. Craciun, C. Galassi, Merging of the polar and tilt

instability lines near the respective morphotropic phase boundaries of $PbZr_{1-x}$ Ti_xO_3, Phys. Rev. B 87 (2013) 094108.
[8] F. Cordero, F. Trequattrini, F. Craciun, C. Galassi, Effects of aging and annealing on the polar and antiferrodistortive components of the antiferroelectric transition in $PbZr_{1-x}$ Ti_xO_3, Phys. Rev. B 89 (2014) 214102.
[9] J.N. Wang, W.L. Li, X.L. Li, W.D. Fei, Rhombohedral-monoclinic phase transition related to grain orientation in Zr-rich $Pb(Zr_xTi_{1-x})O_3$ thin films, J. Alloy. Compd. 509 (2011) 3398–3402.
[10] D.I. Woodward, J. Knudsen, I.M. Reaney, Review of crystal and domain structures in the $PbZr_xTi_{1-x}$ O_3 solid solution, Phys. Rev. B 72 (2005) 104110.
[11] I. Jankowska-Sumara, J. Dec, Phase transitions in $PbZr_{1-x}$ Sn_xO_3, Ferroelectrics 313 (2004) 81–89.
[12] B.S. Toubou, V.G. Smotrakov, O.E. Fesenko, Growth of $PbZr_{1-x}$ $SnxO_3$ single crystals and their phase T, x-diagram, Ferroelectrics 124 (1991) 79–83.
[13] E. Buixaderas, I. Gregora, S. Kamba, J. Petzelt, M. Kosec, Raman spectroscopy and effective dielectric function in PLZT *x*/40/60, J. Phys. Condens. Matter 20 (2008) 345229.
[14] Y.Y. Li, L. Qiang, L. Wang, Z. Yang, X.C. Chu, Growth and characterization of (Pb, La)(Zr, Sn, Ti)O_3 single crystals, J. Cryst. Growth 318 (2011) 860–864.
[15] Z.H. Duan, P. Chang, Z.G. Hu, J.X. Wang, G.S. Wang, X.L. Dong, J.H. Chu, Temperature dependent Raman scattering and far-infrared reflectance spectra of MgO modified $Pb_{0.99}(Zr_{0.95}$ $Ti_{0.05})_{0.98}$ $Nb_{0.02}$ O_3 ceramics: a composition effect, J. Appl. Phys. 116 (2014) 093513.
[16] J. Hlinka, J. Petzelt, S. Kamba, D. Noujni, T. Ostapchuk, Infrared dielectric response of relaxor ferroelectrics, Phase Trans. 79 (2006) 41–78.
[17] P.A. Jansson, Deconvolution with Applications in Spectroscopy, Academic Press, 1984, ISBN 0-12-380220-2.
[18] M. Evans, Nicholas, B. Peacock, Statistical Distributions, John Wiley and Sons, 1993, ISBN 0-471-55951-2, pp. 42–44.
[19] N.L. Johnson, S. Kotz, Continuous Univariate Distributions 1, John Wiley and Sons, 1970, pp. 154–165.
[20] G. Kugel, I. Jankowska-Sumara, K. Roleder, J. Dec, High temperature Raman light scattering in $PbZrO_3$ single crystals, J. Korean Phys. Soc. 32 (1998) S581.
[21] A. Slodczyk, P. Colomban, Probing the nanodomain origin and phase transition mechanisms in (Un)poled PMN-PT single crystals and textured ceramics, Materials 3 (2010) 5007–5028.
[22] A. Slodczyk, P. Colomban, M. Pham-Thi, Role of the TiO_6 octahedra on the ferroelectric and piezoelectric behaviour of the poled $PbMg_{1/3}$ $Nb_{2/3}$ O_{3-x} $PbTiO_3$ (PMN-PT) single crystal and textured ceramic, J. Phys. Chem. Solids 69 (2008) 2503–2513.
[23] I. El-Harrad, C. Carabatos-Nédelec, J. Handerek, Z. Ujma, D. Dmytrow, Low-temperature order-disorder phase transition of PLZT x: 95: 5 ceramics, with La content x=0.5–4% by weight, determined by Raman spectroscopy, J. Raman Spectrosc. 25 (1994) 799–804.
[24] E. Buixaderas, D. Nuzhnyy, J. Petzelt, L. Jin, D. Damjanovic, Polar lattice vibrations and phase transition dynamics in $Pb(Zr_{1-x}$ $Ti_x)O_3$, Phys. Rev. B 84 (2011) 184302.
[25] D. Viehland, J.F. Li, X. Dai, Z. Xu, Structural and property studies of high Zr-content lead zirconate titanate, J. Phys. Chem. Solids 57 (1996) 1545–1554.
[26] P. Ghosez, E. Cockayne, U.V. Waghmare, K.M. Rabe, Lattice dynamics of $BaTiO_3$, $PbTiO_3$, and $PbZrO_3$: A comparative first-principles study, Phys. Rev. B 60 (1999) 836.
[27] M. Deluca, H. Fukumura, N. Tonari, C. Capiani, N. Hasuike, K. Kisoda, C. Galassi, H. Harima, Raman spectroscopic study of phase transitions in undoped morphotropic $PbZr_{1-x}$ Ti_xO_3, J. Raman Spectrosc. 42 (2011) 488–495.
[28] L. Mitoseriu, M.M. Carnasciali, P. Piaggio, P. Nanni, Raman investigation of the composition and temperature-induced phase transition in ceramics, J. Appl. Phys. 96 (2004) 4378.
[29] I. Jankowska-Sumara, Antiferroelectric phase transitions in single crystals $PbZrO_3$: Sn revisited, Phase Trans. 87 (2014) 685–728.